Journal of Applied Spectroscopy, Vol. 80, No. 4, September, 2013 (Russian Original Vol. 80, No. 4, July–August, 2013)

MODELING IR SPECTRA OF URANIUM MONOXIDE CLUSTERS

M. B. Shundalau,[a,*] D. S. Umreiko,[b] A. P. Zazhogin,[a] and A. I. Komyak[a]

UDC 539.19

Structural models were designed and spectral characteristics were computed based on DFT calculations of uranium monoxide clusters $(UO)_2$, $(UO)_4$, $(UO)_6$, and $(UO)_9$. Spectral features that were characteristic of the cluster formation process were identified. The uranium oxidation state was close to 3 in the clusters $(UO)_2$, $(UO)_4$, and $(UO)_6$. The vibrational frequencies decreased monotonically in the sequence $(UO)_2 \rightarrow (UO)_4 \rightarrow (UO)_6$ because of decreasing electron density in each of the UO bonds with the growing complexity of the clusters. The uranium oxidation state was close to 4 in the cluster $(UO)_9$. This led to a strengthening of the bonds and an increase in the frequency of the strongest band in the IR spectrum.

Keywords: *ab initio calculation, density functional theory, effective core potential, infrared spectrum, uranium monoxide, molecular cluster.*

Introduction. Studies during the last decades [1] showed that the monoxide UO can exist along with three previously known uranium oxides (dioxide UO_2, mixed oxide U_3O_8, and trioxide UO_3) in addition to the more complicated species U_2O_3, U_2O_5, U_3O_7, and U_4O_9. It was found that these compounds are not stoichiometric and actually exist as various non-stoichiometric species. Several homogeneous regions with variable U and O composition were detected in the U–O system. It was also hypothesized that several phases, some of which are unstable, exist [1]. An accurate determination of the structures of metastable phases is interesting with respect to technical problems of storage and subsequent disposal of spent nuclear fuel (in particular, UO_2 oxidation in air to U_3O_7 and U_3O_8) [2].

Vibrational IR spectra of the simplest U oxides (neutral UO, UO_2, UO_3, and several ions) were studied for molecular systems isolated in low-temperature matrices of inert gases and nitrogen [3–6]. As a rule, spectral shifts of vibrational frequencies for molecular systems in matrix isolation are known to be small relative to the gas phase [7]. This enables the results of such studies to be interpreted using computations performed for monomeric species of non-interacting molecular systems (i.e., for a gas-phase model). Nevertheless, spectral shifts for matrix isolation can in several instances become significant. Thus, an analysis of vibrational spectra of U mono- and dioxide showed [3, 6] that the long-wavelength (70 and 140 cm^{-1}) shifts of the UO stretching frequencies of these compounds in Ar or Kr matrices were anomalously large compared with those in Ne. It was hypothesized based on the computed electronic structures of these compounds that the isolated molecules interacted strongly with the matrix atoms, leading to a change of the ground electronic term of the molecules [6, 8]. Later [9, 10], this hypothesis was questioned so that the reasons for the aforementioned spectral shifts remain obscure.

Hence it follows that it is difficult to identify separate components of the complicated U–O system even for the simplest U oxides in the molecular form. This is due to the large number of various neutral and ionized ablation products and also their interaction with the environment. In addition to the simplest molecular systems formed under these conditions, more complicated nano-sized clusters can form during the synthesis of U oxides. Model structures of simple U compounds with O and computation of their vibrational spectra can be very useful for determining their structures and compositions [11]. The experimental Raman spectrum of the α-modification of UO_3 was interpreted earlier based on quantum-chemical computations [12].

*To whom correspondence should be addressed.

[a]Belarusian State University, 4 Nezavisimost' Ave., Minsk, 220030, Belarus; e-mail: shundalov@bsu.by; [b]A. N. Sevchenko Institute of Applied Physical Problems, Belarusian State University, Minsk; e-mail: lab_dozator@mail.ru.

Translated from Zhurnal Prikladnoi Spektroskopii, Vol. 80, No. 4, pp. 545–550, July–August, 2013. Original article submitted April 5, 2013.

 0021-9037/13/8004-0530

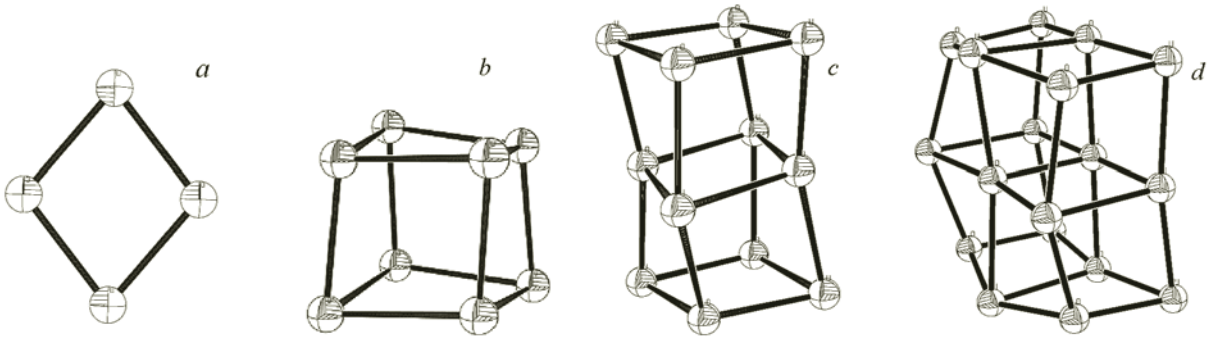

Fig. 1. Structures of clusters $(UO)_2$ (a), $(UO)_4$ (b), $(UO)_6$ (c), and $(UO)_9$ (d).

Herein results from quantum-chemical modeling of the structures and vibrational IR spectra of UO clusters are presented. UO in the crystalline phase has a cubic lattice [1]. Starting from there, monoxide clusters representing fragments of the three-dimensional crystal structure, i.e., $(UO)_2$, $(UO)_4$, $(UO)_6$, and $(UO)_9$, are examined (Fig. 1).

Computations. The applied quantum-chemical program GAMESS-US [13, 14] was used to optimize the equilibrium structure and to compute force fields, eigen frequencies of vibrations and intensities in IR spectrum in the harmonic approximation for UO and the clusters $(UO)_2$, $(UO)_4$, $(UO)_6$, and $(UO)_9$. The programs MacMolPlt [15] and ORTEP [16] were used to visualize the results. The relativistic effective core potential (RECP) approximation LANL2DZ that replaced 78 inner electrons was used for the U atom [17]. A specially developed DZ-basis set for this RECP was used for the remaining U electrons. The O atom was described based on the standard full-electron correlation-consistent basis set of Dunning [18]. The RECP and corresponding basis sets were generated using the Extensible Computational Chemistry Environment Basis Set Database [19–21]. The hybrid exchange-correlated functional B3LYP was also used in all calculations [22–24].

Results and Discussion. The vibrational frequency for UO monomer was determined for low-temperature matrix isolation in Ar, Kr, and Ne. As noted above, this value depended considerably on the environment, varying from 820 cm^{-1} in Ar [3, 5] and 819 cm^{-1} in Kr [3] to 890 cm^{-1} in Ne [6]. An analysis of the electronic absorption spectrum fine structure of $^{238}U^{16}O$ in the gas phase [25] gave a value of the vibrational frequency in the range 840–850 cm^{-1}. Therefore, the value of 860 cm^{-1} that was calculated for the gas phase not only can provide a benchmark for determining spectral shifts of the frequencies upon forming clusters but also for demonstrating the agreement with the experimental value. It is also noteworthy that the approximation used in the computations was used successfully to model the structures and vibrational spectra of U-containing compounds (UO_3, UO_2Cl_2, UO_4, and their complexes) [12, 26, 27].

The simplest cluster of UO was considered to be $(UO)_2$. The cluster was initially shaped as a square. The geometry distorted to a rhombic shape with D_{2h} symmetry during the optimization (Fig. 1a). The UO bond lengths increased from 1.863 Å in the monomer (experimental value 1.838 Å [25]) to 2.143 Å in the cluster. The angle between the bonds to the U atoms was 78.0°. The cluster $(UO)_2$ had six normal modes: $\Gamma = 2A_g + B_{1u} + B_{2u} + B_{3g} + B_{3u}$. Of these, vibrations of B_{1u}, B_{2u}, and B_{3u} symmetry are active in the IR spectrum. The fully symmetric (A_g) vibrations of the cluster were mixed (ν_s 72% + δ_s 28%) with frequency 579 cm^{-1} and in-plane bending with frequency 180 cm^{-1}. Two stretching vibrations of B_{1u} and B_{2u} symmetry with frequencies 539 and 532 cm^{-1} were the strongest (1.00 and 0.33) in the computed IR spectrum (here and later intensities normalized to the maximum intensity of the vibrational band in the examined spectrum are given). The stretching vibration of B_{3g} symmetry with frequency 357 cm^{-1} was inactive in the IR spectrum. Out-of-plane bending of B_{3u} symmetry with frequency 144 cm^{-1} was weak (<0.01). Thus, formation of even the simplest UO cluster led to a reduction of the fully symmetric vibration of UO bonds by 1.5 times; of the asymmetric ones, by 1.6 times.

The next examined model fragment of the crystal was the cluster consisting of four UO molecules, $(UO)_4$. The starting cluster had the shape of a regular cube. Optimization distorted the geometry (Fig. 1b). Each face of the starting cube was a non-planar rhombus. The UO bonds in the $(UO)_4$ cluster lengthened to 2.297 Å. The angles between the bonds to U atoms changed little (79.4°) compared with the cluster $(UO)_2$. Because the maximum possible point-group symmetry of the cluster was T_d (three-fold rotation axes passing through U and O atoms located in opposite vertexes of the cluster), the cluster in terms of this approximation had eight normal modes: $\Gamma = 2A_1 + 2E_1 + F_1 + 3F_2$. As a rule, each of these was a complicated combination of stretching and bending vibrations. Considering that the geometry was optimized and the vibrational spectrum

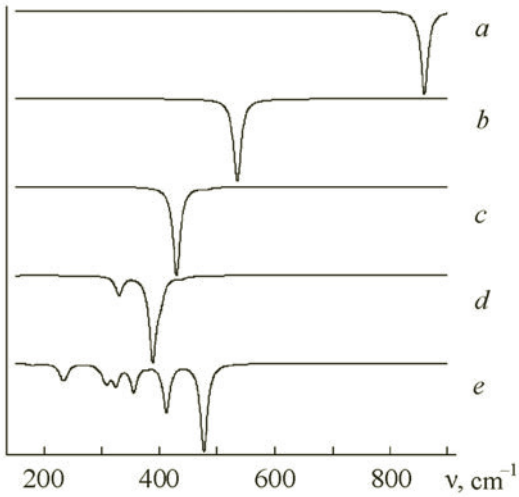

Fig. 2. IR absorption spectra computed in the LANL2DZ/B3LYP/cc-pVDZ approximation of UO monomer (a) and clusters $(UO)_2$ (b), $(UO)_4$ (c), $(UO)_6$ (d), and $(UO)_9$ (e).

was computed in terms of a cluster model of C_{2v} symmetry, the degeneracy was lifted and the frequencies were split. In this instance, the cluster had 18 non-degenerate normal vibrations. Then, returning to the model of higher symmetry and considering the splitting of the vibrational frequencies, we obtained the following distribution of vibrations over symmetry types: A_1, 513 and 185 cm^{-1}; E, (363, 360 cm^{-1}) and (126, 106 cm^{-1}); F_1, (330, 328, 327 cm^{-1}); F_2, (482, 481, 480 cm^{-1}), (431, 430, 428 cm^{-1}), and (138, 137, 133 cm^{-1}). The higher frequencies corresponded to vibrations of the O atom sublattice; lower ones, of the U atoms. In this instance, the assignment of frequencies to definite vibrational types depended considerably on the set of internal vibration coordinates. Thus, the contribution of stretching vibrations to the fully symmetric mode 513 cm^{-1} was 44%; to the three-fold degenerate mode with average frequency 481 cm^{-1}, 96%; etc. for one of the versions of this set (12 stretching and 6 bending coordinates). Only vibrations of type F_2 were resolved in the IR spectrum of the cluster. Of these, only the mode with frequencies 431, 430, and 428 cm^{-1} had non-zero intensity.

It is noteworthy that the UO monomeric species lost their individual features upon combining into clusters. All clusters were in fact new structural units. As a result, analogs of vibrations in the various clusters could be found only based on a correlation of the frequencies, the shifts of which were often difficult to predict, but more likely of the vibrational band intensities and vibration symmetry types. Thus, the relationship of the frequencies and vibration shapes of clusters $(UO)_4$ and $(UO)_2$ was found based on correlations of group symmetry types T_d and D_{2h} and agreement of IR absorption band intensities. Irreducible representation A_1 with this symmetry lowering transforms into A_g and A_2, into A_u. Doubly degenerate representation E decomposes into the sum $A_g + A_u$; triply degenerate representations F_1 and F_2, into $B_{1g} + B_{2g} + B_{3g}$ and $B_{1u} + B_{2u} + B_{3u}$, respectively. Thus, frequency 579 cm^{-1} in $(UO)_2$ decreased to 513 cm^{-1} in $(UO)_4$; 536 cm^{-1}, to 431, 430, 428 cm^{-1}; 532 cm^{-1}, to 482, 481, 480 cm^{-1}; 357 cm^{-1}, to 330, 328, 327 cm^{-1}; 144 cm^{-1}, to 138, 137, 133 cm^{-1}. The analog of the vibration with 180 cm^{-1} in $(UO)_2$ was the mode with frequency 185 cm^{-1} in $(UO)_4$ (Table 1). Figure 2 shows the computed spectra of the monomer and clusters. Thus, formation of a unit cell of UO crystal that contained four atoms each of U and O led to a decrease of the frequency of the fully symmetric vibration of UO bonds by 1.7 times; of antisymmetric vibrations (strong band), by 2 times.

Cluster $(UO)_6$ was initially given a right parallelepiped shape. It had after optimization the shape shown in Fig. 1c and symmetry D_{2h} (two-fold symmetry axis coinciding with the z axis of the fixed molecular coordinate system and passing through the two middle U atoms). This cluster had five different types of UO bonds with lengths 2.252, 2.254, 2.368, 2.376, and 2.497 Å and three types of non-equivalent angles between bonds to U atoms (76.8, 77.6, and 82.7°). The cluster $(UO)_6$ had 30 normal modes: $\Gamma = 6A_g + 2A_u + 3B_{1g} + 5B_{1u} + 3B_{2g} + 4B_{2u} + 3B_{3g} + 4B_{3u}$. Table 1 presents the vibrational frequencies of $(UO)_6$ and their normalized intensities and symmetry types. Where possible, correlations between frequencies and shapes of $(UO)_4$ and $(UO)_6$ cluster vibration shapes were found based on the above concepts. The significant number of non-equivalent geometric parameters (bonds and angles) in $(UO)_6$ was responsible for splitting of the vibrational frequencies. It was noteworthy that the greater part of the corresponding absorption bands had zero or close-to-zero intensity (Table 1). The

TABLE 1. Calculated Characteristic Vibrational IR Spectra of Clusters $(UO)_2$, $(UO)_4$, $(UO)_6$, and $(UO)_9$

$(UO)_2$			$(UO)_4$			$(UO)_6$			$(UO)_9$		
Γ	ν, cm^{-1}	I	Γ	ν, cm^{-1}	I	Γ	ν, cm^{-1}	I	Γ	ν, cm^{-1}	I
A_g	579	0	A_1	513	0	A_g	440	0	A_1	477	1.00
						B_{1u}	439	0.03			
						B_{3g}	407	0			
						B_{2u}	401	0.25			
						A_g	397	0	B_1	437	0
				431		B_{1u}	388	1.00			
B_{1u}	536	1.0	F_2	430	1.00	B_{2u}	386	0.02	E	412	0.28
				428		B_{3u}	383	0.05			
				482		B_{1u}	329	0.13	A_2	340	0
B_{2u}	532	0.33	F_2	481	0.02	B_{2u}	331	0.01	E	355	0.16
				480		B_{3u}	330	0.10			
						B_{2g}	350	0	E	324	0.11
						B_{3g}	346	0			
				363		A_g	323	0	A_1	379	0.02
			E	360	0	A_u	304	0	B_1	359	0
									B_1	339	0
				330							
B_{3g}	357	0	F_1	328	0						
				327							
									B_1	324	0
									B_1	310	0
									E	309	0.06
									A_1	305	0.10
									A_1	297	0.02
									A_1	288	0
									A_1	283	0
						B_{2g}	282	0			
						B_{3u}	238	0.01			
									E	237	0.05
									A_1	231	0.13
						B_{1g}	221	0	A_2	220	0
									E	180	0.01
A_g	180	0	A_1	185	0	A_g	155	0	A_1	142	0.01
						B_{1u}	153	<0.01			
				138		B_{1u}	100	0	A_2	80	0
B_{3u}	144	<0.01	F_2	137	0.01	B_{2u}	119	0	E	88	<0.01
				133		B_{3u}	85	0			
						A_g	126	0	B_1	124	0
									E	122	0
				126		A_g	67	0			
			E	106	0	A_u	51	0	A_1	43	0
						B_{2g}	113	0	E	96	0
						B_{3g}	82	0			
									E	70	<0.01
									E	53	0.02
									B_2	53	0
						B_{1g}	46	0	B_2	51	0
									B_2	30	0
									A_1	29	0
									B_2	19	0
									B_2	15	0

Note. Vibrational spectrum of UO is characterized by wavenumber 860 cm^{-1}; Γ, vibration symmetry type; ν, wavenumber; I, normalized relative intensity.

frequency of the fully symmetric vibration of UO bonds in $(UO)_6$ was about half of that for the monomer; the antisymmetric one (strongest band), 2.2 times less.

Because the valence of the U atoms in $(UO)_2$, $(UO)_4$, and $(UO)_6$ is close to three whereas the number of bonds to each U atom increases as the complexity of the cluster structure increases, the bonds weaken because of redistribution of electron density. As a result, the frequencies of the fully symmetric and strongest antisymmetric vibrations decrease smoothly in the sequence $(UO)_2 \rightarrow (UO)_4 \rightarrow (UO)_6$ (Table 1 and Fig. 2).

The equilibrium configuration of cluster $(UO)_9$ (Fig. 2d) had C_{4v} symmetry (four-fold symmetry axis passing through central O and U atoms). The cluster $(UO)_9$ had seven different types of UO bonds with lengths 2.187, 2.319, 2.368, 2.395, 2.466, 2.536, and 2.580 Å. The angles between bonds to U atoms varied from 74° (for peripheral atoms) to 90° (the atom lying on the C_4 symmetry axis). The cluster $(UO)_9$ had 48 normal modes: $\Gamma = 9A_1 + 3A_2 + 6B_1 + 6B_2 + 12E$. Of these, only A_1 and E were active in the IR spectrum. Correlations of irreducible representations of groups T_d and C_{4v} ($A_1 \rightarrow A_1$; $A_2 \rightarrow B_1$; $E \rightarrow A_1 + B_1$; $F_1 \rightarrow A_2 + E$; $F_2 \rightarrow B_2 + E$) and also D_{2h} and C_{4v} ($A_g \rightarrow A_1$, B_1; $A_u \rightarrow A_1$, B_1; $B_{1g} \rightarrow A_2$, B_2; $B_{1u} \rightarrow A_2$, B_2; $B_{2g} + B_{3g} \rightarrow E$; $B_{2u} + B_{3u} \rightarrow E$) enabled in several instances analogies of normal vibrations of $(UO)_6$ and $(UO)_9$ to be found (Table 1).

The valence of U in $(UO)_9$ was close to four. As a result, the bonds were partially strengthened and the vibrational frequencies increased compared with those in $(UO)_6$. Furthermore, because $(UO)_9$ did not have a center of symmetry, in contrast with the preceding clusters, fully symmetric vibrations, the frequencies of which were greater in all clusters than those of other symmetry types, were active in the IR spectrum. As a result, the frequency of the strongest band in the IR spectrum of $(UO)_9$ was higher than those of $(UO)_4$ and $(UO)_6$. This band decreased by 1.8 times relative to the monomer.

Conclusions. Quantum-chemical modeling in terms of density-functional theory predicted the existence of stable clusters of UO, the compositions of which included from two to nine monomers. Formation of the clusters led to significant lengthening of the UO bonds, which became non-equivalent as the complexity of the cluster structure increased. As a result, vibrational frequencies were split and shifted to the region below 550 cm^{-1}. In contrast with clusters with unsaturated bonds to U, i.e., $(UO)_2$, $(UO)_4$, and $(UO)_6$, the oxidation state of U in $(UO)_9$ was close to four. This led to an increase of the frequency of the strongest band in the IR spectrum. Therefore, it was suggested that the IR spectrum of $(UO)_9$ portrayed most realistically the features of the long-wavelength absorption spectra of such structures. Furthermore, because the first three clusters were examined in terms of models assuming the presence of a center of symmetry, fully symmetric vibrations of such clusters were forbidden in the IR spectrum. In turn, non-degenerate antisymmetric vibrations were forbidden in $(UO)_9$. It could be assumed that high symmetry was not obligatory in this type of actual physical systems. This led to the appearance in the IR spectrum of vibrations, analogs of which were both fully symmetric and antisymmetric modes in the examined model clusters. Characteristic absorption bands could be expected in the region below 480 cm^{-1}.

REFERENCES

1. L. R. Morss, N. M. Edelstein, and J. Fuger (Eds.), *The Chemistry of the Actinide and Transactinide Elements*, 4th edn., Springer, Dordrecht (2006).
2. V. F. Petrunin and A. V. Fedotov, *Scientific Session of MIFI* [in Russian], Moscow, **9**, 198–199 (2006).
3. S. D. Gabelnick, G. T. Reedy, and M. G. Chasanov, *J. Chem. Phys.*, **58**, 4468–4475 (1973).
4. S. D. Gabelnick, G. T. Reedy, and M. G. Chasanov, *J. Chem. Phys.*, **59**, 6397–6404 (1973).
5. R. D. Hunt and L. Andrews, *J. Chem. Phys.*, **98**, 3690–3696 (1993).
6. M. Zhou, L. Andrews, N. Ismail, and C. Marsden, *J. Phys. Chem. A*, **104**, 5495–5502 (2000).
7. A. Barnes, W. J. Orville-Thomas, R. Gaufres, and A. Muller (Eds.), *Matrix Isolation Spectroscopy*, Springer (1981).
8. J. Li, B. E. Bursten, L. Andrews, and C. J. Marsden, *J. Am. Chem. Soc.*, **126**, 3424–3425 (2004).
9. J. Han, V. Goncharov, L. A. Kaledin, A. V. Komissarov, and M. C. Heaven, *J. Chem. Phys.*, **120**, 5155–5163 (2004).
10. L. Gagliardi, M. C. Heaven, J. W. Krogh, and B. O. Roos, *J. Am. Chem. Soc.*, **127**, 86–91 (2005).
11. P. Li, T.-T. Jia, T. Gao, and G. Li, *Chin. Phys. B*, **21**, 043301 (2012).
12. M. B. Shundalau, A. P. Zajogin, A. I. Komiak, A. A. Sokolsky, and D. S. Umreiko, *J. Spectrosc. Dyn.*, **2**, 19 (2012).
13. M. W. Schmidt, K. K. Baldridge, J. A. Boatz, S. T. Elbert, M. S. Gordon, J. H. Jensen, S. Koseki, N. Matsunaga, K. A. Nguyen, S. J. Su, T. L. Windus, M. Dupuis, and J. A. Montgomery, *J. Comput. Chem.*, **14**, 1347–1363 (1993).
14. http://www.msg.ameslab.gov/GAMESS.html
15. B. M. Bode and M. S. Gordon, *J. Mol. Graphics Modell.*, **16**, 133–138 (1998).

16. L. J. Farrugia, *J. Appl. Crystallogr.*, **30**, 565 (1997).
17. L. R. Kahn, P. J. Hay, and R. D. Cowan, *J. Chem. Phys.*, **68**, 2386–2397 (1978).
18. T. H. Dunning, Jr., *J. Chem. Phys.*, **90**, 1007–1023 (1989).
19. https://bse.pnl.gov/bse/portal
20. D. Feller, *J. Comput. Chem.*, **17**, 1571–1586 (1996).
21. K. L. Schuchardt, B. T. Didier, T. Elsethagan, L. Sun, V. Gurumoorthi, J. Chase, J. Li, and T. L. Windus, *J. Chem. Inf. Model.*, **47**, 1045–1052 (2007).
22. A. D. Becke, *J. Chem. Phys.*, **98**, 5648–5652 (1993).
23. C. Lee, W. Yang, and R. G. Parr, *Phys. Rev. B: Condens. Matter Mater. Phys.*, **37**, 785–789 (1988).
24. P. J. Stephens, F. J. Devlin, C. F. Chabalowski, and M. J. Frisch, *J. Phys. Chem.*, **98**, 11623–11627 (1994).
25. L. A. Kaldein and M. C. Heaven, *J. Mol. Spectrosc.*, **185**, 1–7 (1997).
26. M. B. Shundalov, A. I. Komyak, A. P. Zazhogin, and D. S. Umreiko, *Zh. Prikl. Spektrosk.*, **79**, No. 1, 27–36 (2012).
27. M. B. Shundalau, A. I. Komiak, A. P. Zajogin, and D. S. Umreiko, *J. Spectrosc. Dyn.*, **3**, 4 (2013).